Crystallographic Study of Solid Solutions in the Mg-Ca-Nd Ternary System at 400°C

[1]Yogesh Iyer Murthy*, [2]Sumit Gandhi, [3]Abhishek Kumar

[1,2]Department of Civil Engineering, Jaypee University of Engineering and Technology, Guna, India.

[3]Deprtment of Applied Mechanics, Motilal Nehru National Institute of Technology, Allahabad, India

[1]yogesh.murthy@juet.ac.in, [2]sumit.gandhi@juet.ac.in, [3]abhishek@mnnit.ac.in

Abstract

The homogeneity ranges and crystal structures for the binary substitutional solid solutions, Mg_2Ca, $Mg_{41}Nd_5$, and MgNd extending to the ternary system were discovered using X-ray diffraction and scanning electron microscopy. Mg_2Ca and $Mg_{41}Nd_5$ undergo linear substitution where Ca and Nd replace each other, whereas, MgNd generates a complicated substitutional solid solution where Ca replaces both Mg and Nd. Rietveld analysis in conjunction with Pearson's crystal database and XRD were used to determine the solid solubility ranges of the phases present in the main alloys The lattice parameters and site occupancies were studied for these solid solutions. The experimental investigations were carried out using key alloys annealed at 400°C for four weeks. The solubility limit of Nd in Mg_2Ca is 9.0 at.%. The extended solid solubility of Ca in $Mg_{41}Nd_5$ was determined as 3.9 at.% while that of Ca in MgNd was obtained as 8.9 at.%. The phase Mg_3Nd was found to have negligible solubility and further confirmed by Fourier mapping.

Keywords. Mg-Ca-Nd system, SEM, XRD, Rietveld analysis, solid solutions.

1. INTRODUCTION

The two main processes that help magnesium alloys acquire better mechanical characteristics are solid solution hardening and age hardening. Age hardening becomes possible through precipitation from the supersaturated solution if the solubility of the alloying element decreases with a decrease in temperature. Mg content in precipitates should be high. This enables the increase in volume fraction of precipitate thereby reducing the amount of alloying elements [1]. The alloying element should be selected such that it shows sufficient solubility in Mg at high temperatures and shows considerable improvements in mechanical properties as well. Ca is a low-cost, low-density (1.55 g/cm^3) element with the potential for precipitation hardening [2]. Ca has been reported to be effective in promoting the creep resistance of Mg alloys. Through the refining of grain size, the addition of Ca increases ductility [3], and it also increases strength, castability, creep resistance, and corrosion resistance [4]. The addition of Ca has been discovered to make magnesium more resistant to oxidation at temperatures exceeding 480 °C [5] and to raise the ignition temperature of magnesium [6], making magnesium safer for use in aerospace and

automotive applications [7]. The Mg-Ca-based alloys have also lately discovered a wide range of intriguing uses in the realm of biodegradable implant materials [8–11].

One drawback of alloying Mg with Ca alone is that Mg ignition cannot be avoided during melting. Additionally, the Mg-Ca alloy becomes more brittle as the Ca percentage rises [12]. Therefore, the third element, Nd was considered to be added to the Mg-Ca binary system. The addition of Nd is beneficial in the strengthening of Mg alloys. It purifies the alloy melt thus improving castability. According to Xin et al. [13], adding Nd to magnesium results in a more refined solidified microstructure, which enhances the material's mechanical properties by increasing yield strength, tensile strength at high temperatures [13], and oxidation resistance. The addition of rare earth elements such as Nd also improves ductility and corrosion resistance [14] and creep resistance [15]. Furthermore, Mg-Nd based alloys have many applications as biocompatible materials, such as, bioabsorbable implant devices [16,17], cardiovascular implants [17], and orthopedic applications. [18] .

There hasn't been enough research on the Mg-Ca-Nd ternary phase diagrams in the literature as of yet. Recently, Fei *et al*. [19] studied this system at 400°C in the Mg-rich corner using equilibrated alloys. The partial isothermal is re-drawn as shown in Figure 1. Six samples were used to map this section and the locations for these samples are shown in Figure 1. They identified two three-phase triangulations in this region, Mg + Mg_2Ca + $Mg_{41}Nd_5$ and $Mg_{41}Nd_5$ + Mg_2Ca+ Mg_3Nd. They also reported the solubility limit of Ca in $Mg_{41}Nd_5$ to be 3.57 at.%. and that of Nd in Mg_2Ca to be 1.24 at.%.

The present investigation describes the extended homogeneity ranges of the binary compounds in the ternary Mg-Ca-Nd system. Knowledge of phase relationships and solubility limits is important to understand the microstructure and mechanical properties such as tensile strength and ductility of the resulting alloys. The increased homogeneity enables the easier synthesis of the compound. Moreover, properties such as lower density and higher specific strength could be obtained by tailoring the composition.

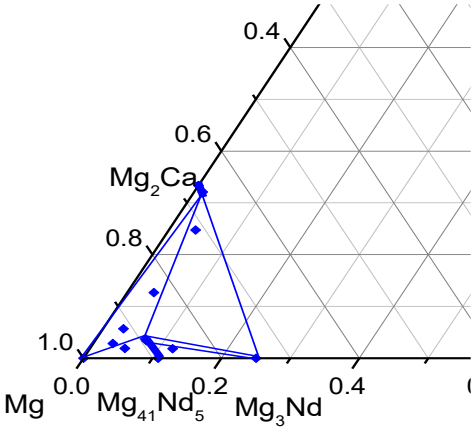

Figure. 1 Partial isothermal section of Mg-Ca-Nd system at 400°C as per Fei *et al* [19]

2. EXPERIMENTAL PROCEDURE

Key alloys were prepared using high purity Mg ingot of 99.8%, Ca with 99%, and Nd with 99.6% all supplied by Alfa Aesar® Company. These samples were initially made using a non-consumable tungsten electrode in an arc-melting furnace that was water cooled in a copper crucible. To ensure uniformity, the samples were crushed and remelted three to four times. Later, the samples were melted at least three times in an induction furnace using Tantalum crucible. To make up for the evaporation losses, extra magnesium (approximately 10 percent) was added. Utilizing an Ultima2 inductively coupled plasma optical emission spectrometer, the exact global composition was discovered (ICP-OES). By averaging the composition of three separate parts from each sample, the true composition was calculated. The deviation the from original composition was found to be negligible in most cases. The actual compositions of the key alloys are shown in Figure 2. The alloys were wrapped in tantalum foils, encapsulated in an argon-purged quartz tube and annealed for four weeks at 400°C. Using a Hitachi S-3400N SEM with EDS, the phase compositions, phase relations, and homogeneity ranges were investigated. With a 2 m probe size, 15 kV accelerating voltage, and 50 nA probe current, samples were analysed.

The XRD patterns were obtained using a PAN analytical X'pert Pro powder X-ray diffractometer with CuKα radiation. The XRD spectrum was acquired from 20 to 90° 2θ with a 0.02° step size. X-ray diffraction study of the samples was carried out using X'Pert High Score Plus Rietveld analysis software. Si was used as an internal calibration standard for correcting the zero shift and specimen surface displacement which are the most serious systematic errors in x-ray powder diffraction patterns. The crystal structure data of the binary compounds were taken from Pearson's crystal structure database [22].

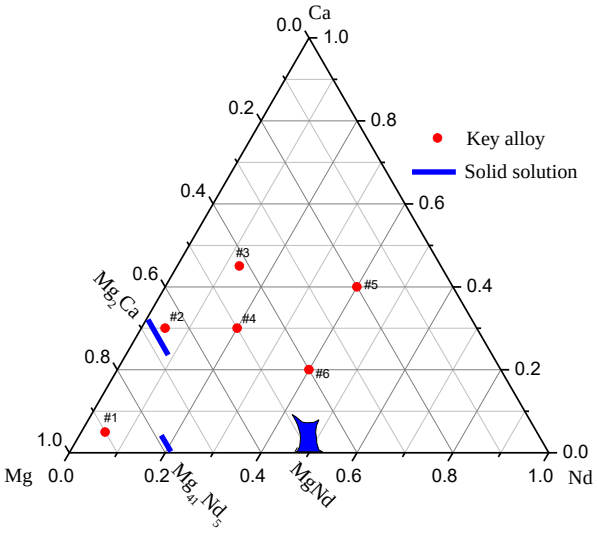

Figure 2. critical alloys' actual compositions and the locations of solid solutions in Gibb's triangle for Mg-Ca-Nd system at 400°C.

3. RESULTS AND DISCUSSION

To study the solubility ranges of the binary compounds, several alloys were prepared and annealed at 400°C for four weeks. The annealed alloys were then quenched in cold water to maintain the microstructure present at the annealing temperature. In the current research, six selected alloys prepared in the ternary system are discussed. The locations of these alloys are shown in Figure 2. The actual composition obtained from ICP and phase identification of the key alloys determined by SEM/EDS and XRD are summarized in Table 1. Figure 3 (a-c) shows the backscatter electron (BSE) images of the sample #1, #2 and #4. To determine the composition of the equilibrated phases and to identify them, the alloys underwent SEM/EDS spot analysis. XRD analysis was performed to identify and to verify the crystal structures of the phases contained in the alloys. The unit cell parameters, lattice volume and phase, composition determined by XRD results are presented in Table 2. The phase relations obtained by SEM/EDS shows great consistency with those obtained by XRD.

Table 1. Actual sample compositions with phase composition determined by XRD results

Sample No.	Actual composition identified by ICP (at %)			Phase identification		Composition of phase by SEM/EDS (at.%)			Composition of phase by Rietveld analysis (at.%)		
	Mg	Ca	Nd	By SEM	By XRD	Mg	Ca	Nd	Mg	Ca	Nd
1	90	5	5	Mg	Mg	100	0	0	100	0	0
				$Mg_2(Ca,Nd)$	$Mg_2(Ca,Nd)$	66.67	31.73	1.6	66.6	31.64	1.7
				$Mg_{41}(Nd,Ca)_5$	$Mg_{41}(Nd,Ca)_5$	88.85	3.83	7.32	88.6	3.85	7.47
2	65	30	5	$Mg_{41}(Nd,Ca)_5$	$Mg_{41}(Nd,Ca)_5$	89.14	2.01	8.85	88.5	1.8	9.7
				$Mg_2(Ca,Nd)$	$Mg_2(Ca,Nd)$	65.57	31.63	2.8	66.6	30.67	2.66
				$Mg_3(Nd,Ca)$	$Mg_3(Nd,Ca)$	75.0	1.0	24.0	75.0	1.0	24.0
3	42	45	13	Mg(Nd,Ca)	Mg(Nd,Ca)	47.62	8.69	43.70	48	8.5	43.5
				$Mg_2(Ca,Nd)$	$Mg_2(Ca,Nd)$	65.46	25.58	8.96	66.6	24.33	9.0
				Ca	Ca	0	100	0	0	100	0
				Mg(Nd,Ca)	Mg(Nd,Ca)	49.13	8.60	42.27	48	8.5	43.5
4	50	30	20	Ca	Ca	0	100	0	0	100	0
				$Mg_2(Ca,Nd)$	$Mg_2(Ca,Nd)$	66.67	24.63	8.7	66.6	24.33	9.0
				Mg(Nd,Ca)	Mg(Nd,Ca)	47.76	7.48	44.76	48	7.5	44.5
5	20	40	40	Ca	Ca	0	100	0	0	100	0
				(Nd)	(Nd)	0	0	100	0	0	100
6	40	20	40	Mg(Nd,Ca)	Mg(Nd,Ca)	47.66	7.50	44.85	48	7	45
				Ca	Ca	0	100	0	0	100	0

3.1 Solubility *study of Mg_2Ca phase*

The binary Mg_2Ca has the C14 type hexagonal structure [22] with *$P6_3/mmc$* (194) space group and the Pearson symbol is hP12. It has a $MgZn_2$ prototype with 12 atoms in the

primitive unit cell where Ca atoms in the 4f Wyckoff position and Mg atoms on 2a and 6h Wyckoff sites. The atomic coordinates are 4f (0.333,0.667,0.562), 2a (0,0,0) and 6h (0.169,0.338,0.250). The EDS spot analysis revealed the substitution of Ca by Nd at constant Mg concentration of 66.67 at. %. Rietveld analysis of the samples annealed at 400°C for four weeks also shows that, Mg_2Ca forms a linear substitutional solid solution where Nd replaces Ca in 4f position and the Mg concentration remains constant. In order to understand this mechanism of substitution and the maximum and minimum solubilities of Nd in Ca, key alloys #1, #2 and #3 were prepared. The XRD patterns of these alloys are presented in Figure 4. The key alloy #1 is in a three-phase region consisting of $Mg+Mg_2Ca+Mg_{41}Nd_5$. Figure 3(a) shows the SEM micrograph of this sample. The solubility of Nd in Mg_2Ca for sample #1 was obtained as 1.6 at.%. This value is consistent with those reported by Fei *et al.* [19], who reported the solubility value as 1.24 at.%. SEM micrograph of the key alloy #2 is presented in Figure 3 (b). This alloy is also located in a three-phase region: $Mg_{41}Nd_5$ + Mg_2Ca+ Mg_3Nd. The solubility of Nd in Mg_2Ca was determined to be 2.8 at.%. Figure 3 (c) shows the BSE image of sample #3. The key alloys #3 and #4 are present in the same triangulation Mg_2Ca+Ca+MgNd and show consistent solubility values. The solubility limit of Nd in Mg_2Ca is found to be 8.56 at. % by SEM and 9.0 at.% by Rietveld analysis and is given by key alloys #3 and #4. The values of unit cell parameters and lattice volume are presented in Table 2.

The characteristics of the unit cell are reduced by replacing Ca with Nd, which has a slightly smaller atomic radius. This is clearly indicated by the shifting of peaks towards higher 2θ values from sample 1 to 3 following the Bragg's Law (Figure 4). In addition, the values of lattice parameters are compared with the standard values of the lattice parameters of Mg_2Ca binary compound taken from Pearson's crystal database [22]. The linear variation of lattice parameters of Mg_2Ca and occupancy of Ca with decreasing concentrations of Ca is presented in Figure 5. Least square approximation was used to establish the relations between unit cell parameters and Ca concentration. The substitution of Ca by Nd is found to be linear obeying the Vegard's Law, thereby clearly indicating the formation of substitutional solid solution. Table 3 describes the refined crystal structure parameters, the occupancies and the reliability factors of all the solid solutions present in the system. The decrease in the value of the reliability factors is also in favour of the well refined unit cell parameters. The coordination spheres and dynamic atomic substitution of Ca by Nd in the 4f Wyckoff position is shown schematically in Figure 6.

Table 2. Actual sample compositions with unit cell parameters, lattice volume and phase composition determined by XRD results.

Sample No.	Actual composition identified by ICP (at.%)			Phase identification	Unit cell parameters and lattice volume		
	Mg	Ca	Nd		*a*(Å)	*c*(Å)	Vol.(Å^3)
1	90	5	5	Mg	3.223	5.219	46.950
				$Mg_2(Ca,Nd)$	6.24	10.123	341.357
				$Mg_{41}(Nd,Ca)_5$	14.803	10.422	2283.96
2	65	30	5	$Mg_{41}(Nd,Ca)_5$	14.789	10.411	2276.72

				$Mg_2(Ca,Nd)$	6.228	10.037	333.485
				$Mg_3(Nd,Ca)$	7.399	7.399	405.060
3	42	45	13	Mg(Nd,Ca)	3.884	3.884	58.592
				$Mg_2(Ca,Nd)$	6.194	10.037	333.485
				Ca	5.479	5.479	164.476
4	50	30	20	Mg(Nd,Ca)	3.884	3.884	58.592
				Ca	5.479	5.479	164.476
				$Mg_2(Ca,Nd)$	6.194	10.037	333.485
5	20	40	40	Mg(Nd,Ca)	3.880	3.880	58.411
				Ca	5.479	5.479	164.476
				(Nd)	3.659	11.796	136.770
6	40	20	40	Mg(Nd,Ca)	3.879	3.879	58.366
				Ca	5.479	5.479	164.476

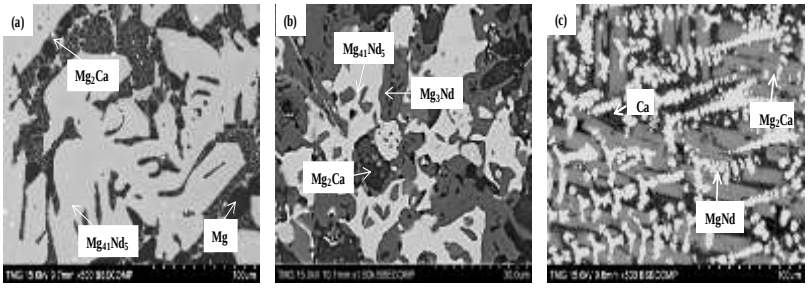

Figure 3. (a-c). BSE images of alloy #1, #2 and #3 all annealed at 400°C for four weeks.

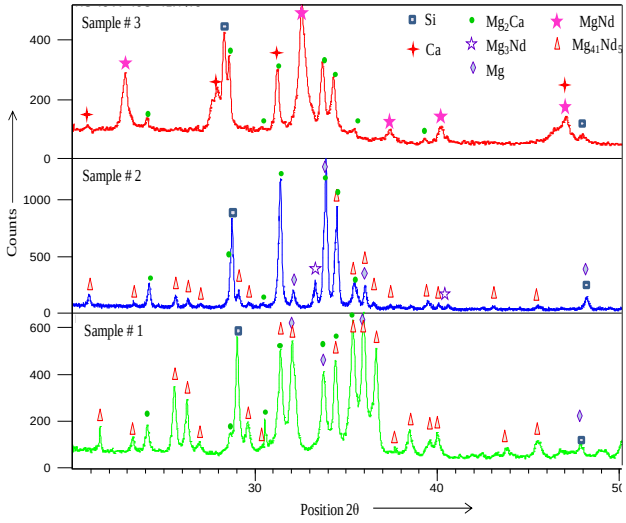

Figure 4. XRD pattern of key alloy #1, #2 and #3 all annealed at 400°C for four weeks.

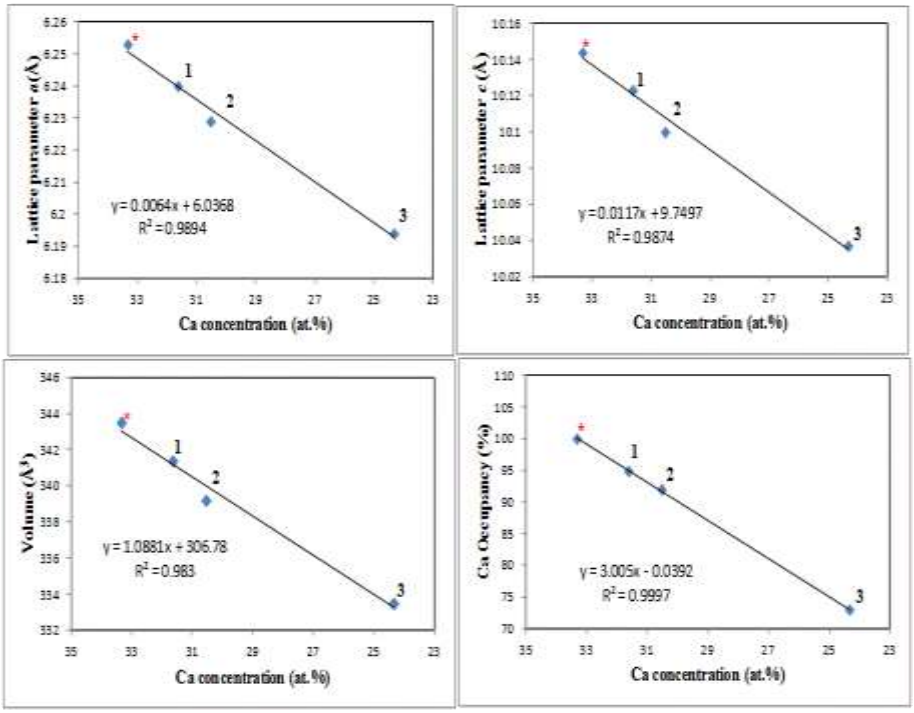

Figure 5. Variation of lattice parameters and occupancy for Mg_2Ca with Ca concentration where progressive substitution of Ca by Nd decreases the cell parameters *a*, *c* and volume and Occupancy of Ca.

* Values obtain by Mg_2Ca binary compound from Pearson's Crystal structure database [21]

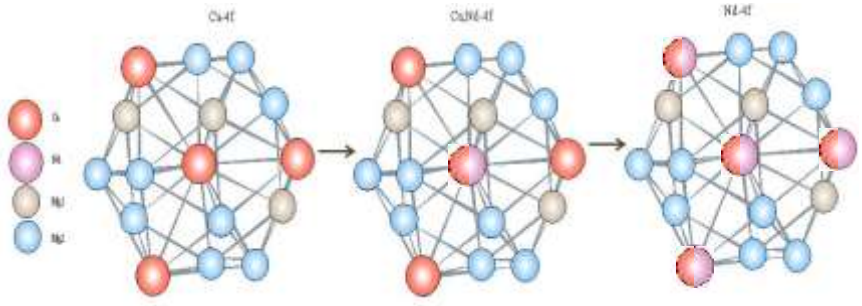

Figure 6. The coordination spheres of dynamic atomic substitution of Ca by Nd in the 4f atomic coordinates

Table 3. Refined crystal structure parameters of the solid solutions.

Sample No.	Phase	Wyckoff position		Occupancy (%)	Reliability Factors*		
					R_e	R_{wp}	*s*
1	$Mg_2(Ca,Nd)$	Mg1	2a	100	11.84	16.68	1.98
		Mg2	6h	100			
		Ca	4f	94.9			
	$Mg_{41}(Nd,Ca)_5$	Mg1	16i	100			
		Mg2	16i	100			
		Mg3	16i	100			
		Mg4	8h	100			
		Mg5	8h	100			
		Mg6	8h	100			
		Nd1	8h	100			
		Mg7	8f	100			
		Mg8	2a	100			
		Nd2	2a	34.4			
2	$Mg_2(Ca,Nd)$	Mg1	2a	100	12.38	13.47	1.18
		Mg2	6h	100			
		Ca	4f	92			
	$Mg_{41}(Nd,Ca)_5$	Mg1	16i	100			
		Mg2	16i	100			
		Mg3	16i	100			
		Mg4	8h	100			
		Mg5	8h	100			
		Mg6	8h	100			
		Nd1	8h	100			
		Mg7	8f	100			
		Mg8	2a	100			
		Nd2	2a	50			
3	$Mg_2(Ca,Nd)$	Mg1	2a	100	11.69	13.25	1.28
		Mg2	6h	100			
		Ca	4f	73			
	Mg(Nd,Ca)	Nd	1b	84			
		Mg	1a	96			
4	$Mg_2(Ca,Nd)$	Mg1	2a	100	15.31	16.46	1.16
		Mg2	6h	100			
		Ca	4f	81			
	Mg(Nd,Ca)	Nd	1b	90			
		Mg	1a	96			
5	Mg(Nd,Ca)	Nd	1b	90	15.25	16.52	1.17
		Mg	1a	96			
6	Mg(Nd,Ca)	Nd	1b	94.7	13.01	21.84	2.82
		Mg	1a	95.5			

*Reliability factors: *s* is the goodness of fit, *Rwp* is the weighted summation of the residuals of the least-squares fit and *Re* is the statistically expected value.

3.2 Solubility study of $Mg_{41}Nd_5$ phase

In the Mg-Nd binary system, $Mg_{41}Nd_5$ is the richest binary compound in Mg content. Like other $Mg_{41}RE_5$ phases, it has a tetragonal structure (tI92-Ce_5Mg_{41} type) [1]. $Mg_{41}Nd_5$ has 92 atoms in the unit cell as presented in Table 2. Key alloy #1 and #2, which were used for the solubility study of Mg_2Ca could also be used for the study of solubility limits of $Mg_{41}Nd_5$.

Similar to Mg_2Ca, $Mg_{41}Nd_5$ also undergoes linear solid substitution, where Ca substitutes Nd in the 2a (0,0,0) position.

The key alloy #1 was determined to be in a three-phase region Mg + Mg_2Ca + $Mg_{41}Nd_5$. The maximum solubility of Ca in $Mg_{41}Nd_5$ is found to be 3.83 at. % by SEM and 3.85 at.% by Rietveld analysis. This value of solubility was found consistent with that of Fei *et al*. [19], who reported the value to be 3.57 at.%. The key alloy #2 also belongs to a three-phase region $Mg_{41}Nd_5$ + Mg_2Ca + Mg_3Nd as discussed previously, yielding a solubility value of Ca of 2.8 at.%. The XRD pattern for the two key samples is shown in Figure 4. In this case, there is a slight shifting of peaks towards lower values of 2θ with the increase in Ca content. This could be explained from the fact that, since Ca atoms are slightly larger than Nd, their substitution results in increasing the interplanar distance, hence resulting in peak shifts towards lower values of 2θ in accordance with Bragg's Law. The values of lattice parameters are presented in Table 2 and their variation with Nd concentration is shown in Figure 7. The dynamic substitution of Nd by Ca in the 2a Wyckoff position is presented in Figure. 8.

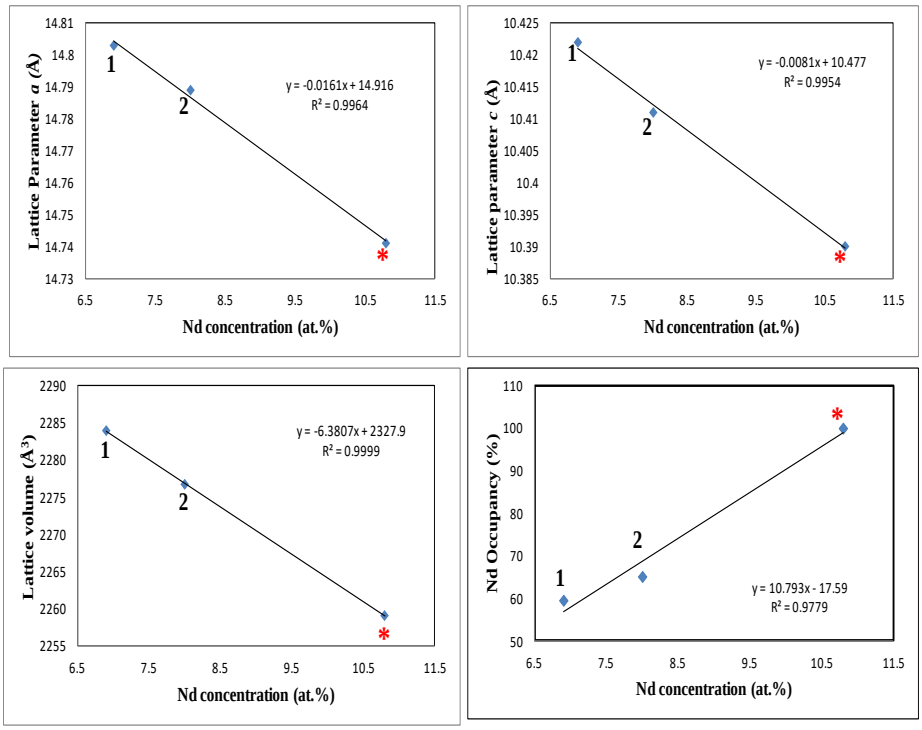

Figure 7. Variation of lattice parameters and occupancy with Nd concentration where progressive substitution of Nd by Ca decreases the cell parameters *a*, *c* and volume and increase the occupancy of Nd.

* Values obtain by $Mg_{41}Nd_5$ binary compound from Pearson's Crystal structure database [21]

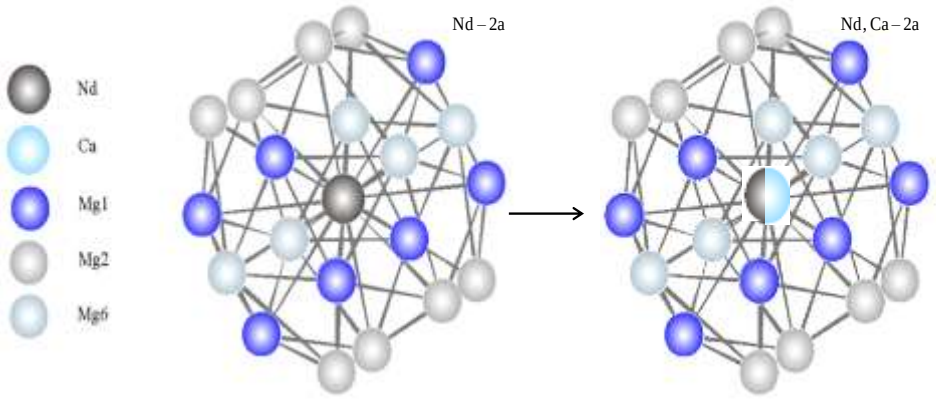

Figure 8. The coordination spheres of dynamic atomic substitution of Nd by Ca in the 2a atomic coordinates

3.3 Solubility study of MgNd phase

The MgNd phase has a ClCs prototype with cubic crystal structure and Pm-3m (221) space group [1]. It has Mg in 1a position with coordinates (0,0,0) and Nd in 1b position with coordinates (0.50,0.50,0.50). This is the only binary phase in this ternary system which undergoes complex substitution, where Ca replaces both Mg of 1a position and Nd of 1b position. Key alloys #4, #5 and #6 were used to study this complex solid solution. Figure 9 shows Rietveld analysis of key alloy #4, #5 and #6 all annealed at 400°C for four weeks.

The key alloy #4 is located in a three-phase region of Mg_2Ca + MgNd + Ca. From this key alloy, the maximum solubility limit of both Nd in Mg_2Ca and Ca in MgNd were established. The maximum solubility limit of Ca in MgNd in this region was found to be 8.6 at. % (Table 1). The key alloy #5 also represents a three-phase region MgNd + Ca + (Nd). This alloy gives the solubility limit of Ca in MgNd to be 6.8 at.% in the Nd rich side of the ternary phase diagram. In addition, the key alloy #6 is in a two-phase region of Ca and MgNd. The solubility of Ca in this region is obtained as 7.5 at. % showing tie-line relationship of the two phases: Ca and MgNd. From the SEM/EDS results and Rietveld analysis of key alloys #4, #5 and #6 (Table 1), it could be verified that with the addition of Ca atoms, the concentrations of both Mg and Nd decrease. Since the atomic size of Ca is larger than both Mg and Nd, there is an increase in volume and lattice parameter *a* with an increase in Ca concentration. The dynamic substitution of Mg and Nd are represented in Figure 10.

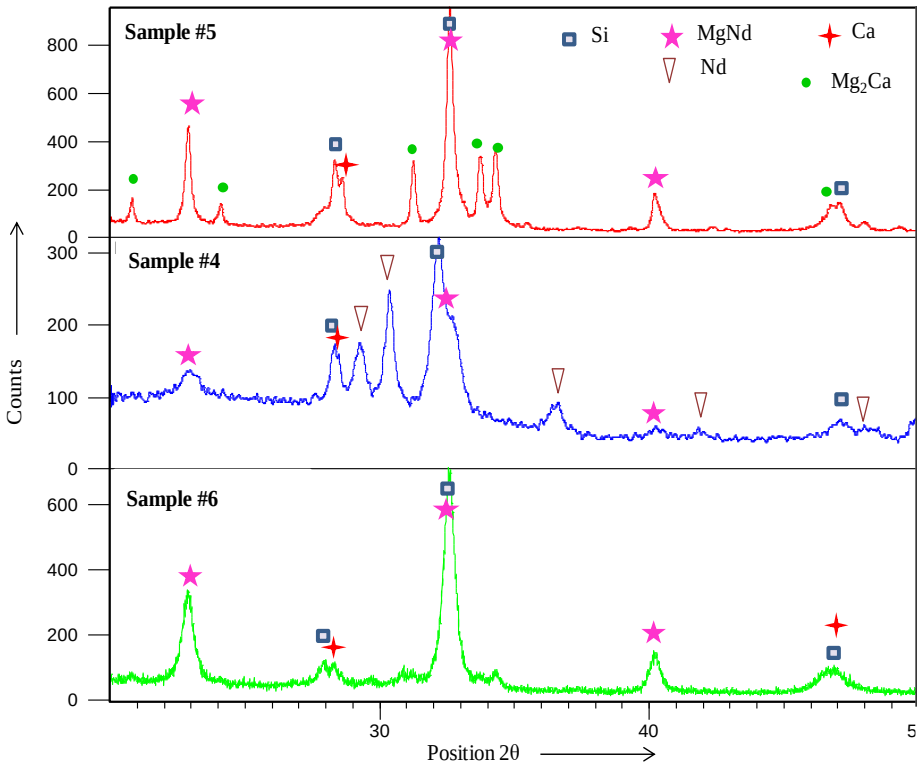

Figure 9. XRD pattern of key alloy #5, #4 and #6 all annealed at 400°C for four weeks

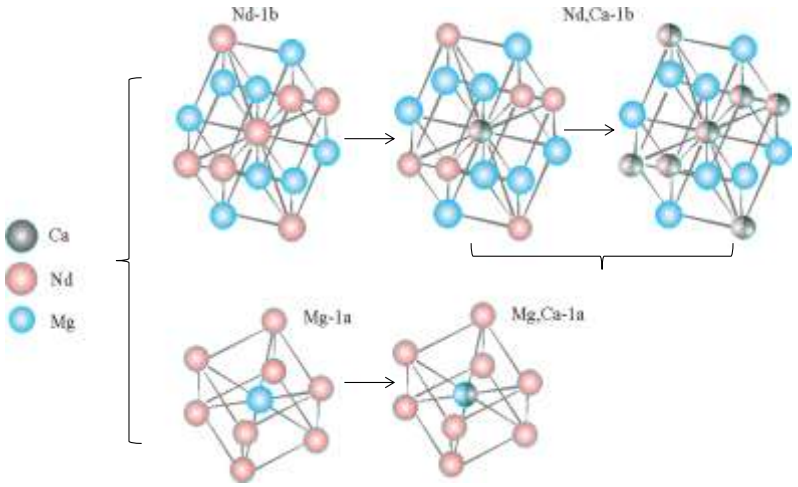

Figure 10. The coordination spheres of dynamic atomic substitution of Ca by Nd with different atomic coordinates

3.4 The Mg_3Nd phase

The Mg_3Nd phase has a BiF_3 prototype with cubic crystal structure and Fd-3m (225) space group [1]. It has Mg1 in 4b position with coordinates (0.50,0.50,0.50), Mg2 in 8c position with coordinates (0.25,0.25,0.25) and Nd in 4a position with coordinates (0,0,0). The phase Mg_3Nd was found to have negligible solubility of Ca in it. For example, in key alloy #2, the solubility of Ca was found to be 1.0 at.% in Mg_3Nd (Table 2), which is within the instrumental error of SEM/EDS. These results are in confirmation with those of Fei *et al*. [19], who found the solubility of Ca in this phase at 0.24 at.%. XRD patterns of key alloy #2 also confirms that there is no shifting of peaks or changes in lattice parameters for this phase. The sliced section of Fourier difference map of Mg_3Nd at all possible atomic coordinates at [0 1 0] plane for key alloy #2 is presented in Figure 11. The Wyckoff position, section and coordinate details are presented in table 4. The Figure 11a shows the Mg1-4b atomic site which was sliced at y = 0.50 level, where the electron density for this position was expected to be maximum. Similarly, the Mg2 and Nd sites were sliced at y = 0.25 (Figure 11b) and y = 0.0 (Figure 11c) levels, respectively. The uniform distribution of electron densities at these positions clearly indicated the absence of any substitution.

Table 4. Wyckoff position, coordinates and slicing levels for Fourier maps of Mg_3Nd

Wyckoff position	**coordinates**			**slicing level**
	x	*y*	*z*	
Mg1-4b	0.50	0.50	0.50	y = 0.50
Mg2-8c	0.25	0.25	0.25	y = 0.25
Nd-4a	0	0	0	y = 0.0

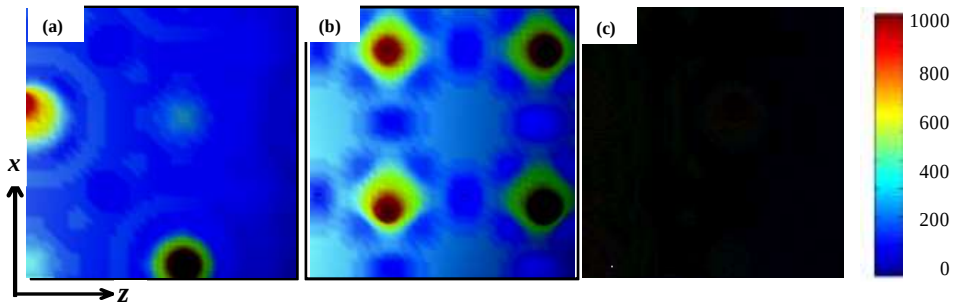

Figure 11. (*a-c*). Fourier maps of Mg_3Nd at (a) Mg1 (b) Mg2 and (c) Nd atomic coordinates.

4. SUMMARY

SEM/EDS and XRD were used to investigate the homogeneity ranges of three binary compounds in the Mg-Ca-Nd system, extending to ternary. The XRD pattern of the six annealed alloys was carried out by Rietveld analysis. In case of Mg_2Ca and $Mg_{41}Nd_5$, linear substitutions were formed and their lattice parameters were found to obey the Vegard's law. MgNd was found to form complex substitutional solid solution, while Mg_3Nd had negligible solubility. The extended solubilities of the binary compounds as obtained from the SEM/EDS spot analysis were found consistent with those obtained from the Rietveld analysis. The dynamic substitution at different atomic coordinates by the substituting atoms in the coordination spheres is also presented. Based on these results, the solubility limits of these compounds extending to the ternary are established.

ACKNOWLEDGEMENT

The authors would like to acknowledge the financial support provided by NSERC.

REFERENCES

[1] S. Delfino, A. Saccone and R. Ferro, "Phase relationships in the neodymium-magnesium alloy system," *Journal of Metallurgical Transactions A*, vol. 21, p. 2109−2114, 1990.

[2] B.L. Mordike and T. Ebert, "Mg Properties — applications — potential," *Materials Science and Engineering A*, vol. 302, pp. 37–45, 2001.

[3] O. Beffort and Ch. Hausmann, "The Influence of Ca-additions on the Mechanical Properties of T300-C-Fibre/Mg (Al) Metal Matrix Composites," *Mg Alloys and their Applications*, pp. 215–220, 2000.

[4] Y.N. Zhang, X. D. Liu, Z. Altounian and M. Medraj, "Coherent nano-scale ternary precipitates in crystallized $Ca_4Mg_{72}Zn_{24}$ metallic glass," *Scripta Materialia*, vol. 68, p. 647-650, 2013.

[5] Y.N. Zhang, D. Kevorkov, F. Bridier and M. Medraj, "Experimental investigation of the Ca-Mg-Zn system using diffusion couples and key alloys," *Journal of Science and Technology of Advanced Materials*, vol. 12, p.1-13, 2011.

[6] A. A. Luo, "Recent Mg Alloys Development for Elevated Temperature Application," *International Materials Review*, vol. 49, pp. 13-30, 2004.

[7] B.S. You, W.W. Park and I. S. Chung, "The effect of Ca additions on the oxidation behavior in Mg alloys," *Scripta Materialia*, vol. 42, pp. 1089–1094, 2000.

[8] I. Polmear, Ed., *Light Alloys from Traditional Alloys to Nano-crystals*. Butterworth-Heinemann, Oxford, UK 2006.

[9] H. Watari, "Japanese Science and Technology Quarterly Report," 2006.

[10] Y.F. Zheng, X.N. Gu, Y. L. Xi and D.L. Chai, "In vitro degradation and cytotoxicity of Mg/Ca composites produced by powder metallurgy," *Acta Biomateriala*, vol. 6, pp. 1783- 91, 2010.

[11] W. Yizao, X Guangyao, L. Honglin, H. Fang, H. Yuan and Z. Xiaoshong, "Preparation and characterization of a new biomedical Mg–Ca alloy," *Materials and Design*, vol. 29, pp. 2034–37, 2008.

[12] L. Zijian, G Xunan, L. Siquan and Z. Yufeng, "The development of binary Mg–Ca alloys for use as biodegradable materials within bone," *Biomaterials,* vol. 29, pp. 1329- 1344, 2008.
[13] I. Antoniac and M. Dinu, "Microstructural and Mechanical Features of Mg-Ca Alloys," in *3rd International Conference on E-Health and Bioengineering*, 2011.
[14] P.J. Li, B. Tang and E.G.Kandalova, "Microstructure and properties of AZ91D alloy with Ca additions," *Journal of materials,* vol. 59, p. 671−675, 2005.
[15] Z. Jinwang, W. Shebin, Z. Junyuan, Z. Jinling and X. Bingshe, "Effects of Nd on Microstructures and Mechanical Properties of AM60 Magnesium Alloy in Vacuum Melting," *Rare Metal Materials and Engineering*, vol. 38, p. 1141−45, 2009.
[16] S. Gorsse, C.R. Hutchinson, B. Chevalier and J.F. Nie, "A thermodynamic assessment of the Mg–Nd binary system using random solution and associate models for the liquid phase," *Journal of Alloys and Compounds,* vol. 392, pp. 253–262, 2005.
[17] F.V. Fanjul, S. Srimanosaowapak, K.R. McNee, G.W. Greenwood and H. Jones, "The effect of Nd substitution for mischmetal on creep performance of Mg-2.5 RE-0.35 Zn-0.3 Mn-0.03 Zr alloy," *Zeitschrift fuer Metallkunde,* vol. 94, pp. 25-29, 2003.
[18] J.M. Seitz, R. Eifler, J. Stahl, M. Kietzmann and W. Bach, "Characterization of MgNd2 alloy for potential applications in bio-resorb able implantable devices," *Acta Biomaterialia,* pp. 1-13, 2012.
[19] H.Fei, L.Liu, H. Bo, L. Zeng and C. Chen, "Phase equilibria in Mg-rich corner of Mg−Ca−RE (RE=Gd, Nd) systems at 400 °C," *Transactions of Nonferrous Metals Society of China*, vol. 23, p. 881−888, 2013.
[20] A. Ulrich, N. Ott, A. Tournier-Fillon, N. Homazava and P. Schmutz, "Investigation of corrosion behavior of biodegradable magnesium alloys using an online-micro-flow capillary flow injection inductively coupled plasma mass spectrometry setup with electrochemical control," *Spectrochimica Acta Part B,* vol. 66, pp. 536–45, 2011.
[21] F. Witte, V. Kaese, H. Haferkamp, E. Switzer, A. MeyerLindenberg, C. J. Wirth and H. Windhagen, "In vivo corrosion of four magnesium alloys and the associated bone response " *Biomaterials,* vol. 26, pp. 3557–63, 2005.
[22] H. Putz, K. Brandenburg, Pearson's Crystal Data, Crystal Structure Database for Inorganic Compounds, CD-ROM software version 1.3.

Biographies

Dr. Yogesh Iyer Murthy pursued his B.E. (Civil Engineering) from DSCE, Bangaluru and M.E. (Structural Engineering) from SGSITS, Indore. He has worked with L&T ECC as Sr. Bridge Engineer (Chennai Division) and has five years of industrial experience before coming into the academics. He has served various engineering colleges for nearly 12 years teaching UG and PG courses in Civil/Structural engineering and has 2.5 years of international R&D experience as research assistant at the thermodynamics of materials

group (TMG), Department of Mechanical and Industrial Engineering, Concordia University, Montreal, Canada. Mr. Murthy has filed for three patents on newer materials in construction industry.

Dr. Abhishek Kumar pursued his B.Tech. (Industrial and Production Engineering) from MIET, Meerut and M.Tech. (Material Science) from MNNIT, Allahabad. He then obtained his PhD degree from IIT Roorkee in the field of Microwave Absorbing Materials in the year 2014. The major areas of his research interest include mechanical behavior of materials, microwave absorbing coatings, dispersed polymers, nano materials and high entropy alloys. He is serving as a reviewer in many reputed journals. Dr. Abhishek has nearly 15 years of teaching experience.

Dr. Sumit Gandhi presently works as an Associate Professor and Head in the Department of Civil Engineering at JUET Guna MP, India. Prior to this he has completed his Ph.D from MNNIT, Allahabad in 2009 in the field of Hydraulic Engineering. He has completed M.Tech from MNNIT Allahabad in 2004 and B.Tech (Civil Engineering) from NMU Jalgaon in 2001. The major areas of his research includes corrugated bed flow, flow over spillways and concrete technology. He is associated with many renowned International Journals as reviewer/editorial board member; and reviewed many research articles and book chapters. He has nearly 15 years of teaching and research experience and also published book & research papers in various journals of repute. Dr. Gandhi has filed two patents.